USING BUILDING AND BRIDGE INFORMATION FOR ADAPTING ROADS TO ALS DATA BY MEANS OF NETWORK SNAKES

Jens Goepfert and Franz Rottensteiner

Institute of Photogrammetry and GeoInformation, Leibniz University Hannover,
Nienburger Strasse 1, 30167 Hannover, Germany – {goepfert, rottensteiner}@ipi.uni-hannover.de

Commission III, WG III/2

KEY WORDS: bridges, buildings, snakes, networks, vector data, roads, ALS, intensity, topology, consistency

ABSTRACT:

In the German Authoritative Topographic Cartographic Information System (ATKIS), the 2D positions and the heights of objects such as roads are stored separately in the digital landscape model (DLM) and digital terrain model (DTM), which is often acquired by airborne laser scanning (ALS). However, an increasing number of applications require a combined processing and visualization of these two data sets. Due to different kinds of acquisition, processing, and modelling discrepancies exist between the DTM and DLM and thus a simple integration may lead to semantically incorrect 3D objects. For example, roads may be situated on strongly tilted DTM parts and rivers sometimes flow uphill. In this paper we propose an algorithm for the adaptation of 2D road centrelines to ALS data by means of network snakes. Generally, the image energy for the snakes is defined based on ALS intensity and height information and derived products. Additionally, buildings and bridges as strong features in height data are exploited in order to support the road adaptation process. Extracted buildings as priors modified by a distance transform are used to create a force of repulsion for the road vectors integrated in the image energy. In contrast, bridges give strong evidence for the correct road position in the height data. Therefore, the image energy is adapted for the bridge points. For that purpose bridge detection in the DTM is performed starting from an approximate position using template matching. Examples are given which apply the concept of network-snakes with new image energy for the adaptation of road networks to ALS data taking advantage of the prior known topology.

1. INTRODUCTION

1.1 Motivation

The German Authoritative Topographic Cartographic Information System (ATKIS®) consists of the digital landscape model (DLM) and the digital terrain model (DTM). The DLM describes the objects on the earth's surface using 2D vector data and additional attributes, whereas the DTM is a continuous 2.5D representation of the surface modelled by terrain points in a regular grid or triangulated irregular network (TIN). For many applications, e.g. flood risk assessment, 3D modelling of the topographic objects is required. For this purpose an integration of the 2D vector data and the height information is necessary. However, there are discrepancies between the DLM and the DTM due to different methods of acquisition, processing, and modelling. As a consequence, integration without matching the data sets leads to semantically incorrect results, e.g. bodies of standing water having physically impossible height variations. Thus, the two data sets have to be adapted for accurate combined visualization and processing.

The terrain data used in the paper are collected by the surveying authority of Schleswig-Holstein by Airborne Laserscanning (ALS). ALS delivers a digital surface model (DSM), from which the DTM is generated by filtering methods. The DSM also contains information about objects situated on the terrain. In addition, ALS data contain the intensity of the reflected signal. Vector data adapted to the ALS data should also match the DTM. We are mainly interested in roads, which typically have an accuracy of 3-5 m in ATKIS, with local deviations that may reach 10 m. It is the goal of this paper to present a new algorithm for improving 2D road vector data using ALS data. The method is based on our previous work in which we used network snakes (Butenuth, 2008) and a task-specific formulation of the image energies for that purpose (Goepfert & Rottensteiner, 2009). In this paper we improve the definition of the image energy, expanding it by terms considering information about bridges and buildings to make it more generally applicable. The new definition of the image energy terms is described, which includes the description of a new method for detecting bridges, and the method is evaluated for an area in Schleswig-Holstein, showing how the accuracy of the road centre lines can be improved.

1.2 Related Work

Pilouk (1996) and Lenk (2001) investigated the incorporation of the 2D geometry of the vector objects into a DTM modelled by a TIN, but the inconsistencies between the vector data and the DTM were not considered. Rousseaux and Bonin (2003) model 2D linear objects such as roads and dikes as 2.5D surfaces by using attributes of the GIS data base and the DTM heights with the goal of generating an improved DTM. They use slopes and regularization constraints to check the semantic correctness of the objects, but they do not adapt the objects if this check fails. Koch (2006) extends the integration methods based on TIN structures by a least squares adjustment using equality and inequality constraints in order to incorporate the semantics of the objects. However, his approach is very sensitive to the definition of the weights if the position and the height observations are corrected simultaneously. Furthermore, the implicit information about the vector objects in the height data such as structure lines at road embankments is not considered. In this paper these deficits are tackled by using the ALS data as image energy for active contours in order to correct the position of the objects considering their height information.

Snakes or parametric active contours are a well-known concept for combining feature extraction and geometric object representation (Kass et al., 1988; Blake & Isard, 1998). They explicitly represent a curve with respect to its arc length. In the standard formulation they cannot handle changes in the topology such as splitting and merging of entities (McInerny & Terzopoulos, 1995). This is not a problem for the adaptation of the 2D vector data to ALS features, because the initial topology is taken from the GIS data base and should be held fixed during the process. For that reason the network-snake algorithm of Butenuth (2008) is used with new definitions of the image energy functions. The basic concept of snakes is widely used in image and point cloud analysis as well as GIS applications. For example, Burghardt and Meier (1997) suggest an active contour algorithm for feature displacement in automated map generalisation, and Cohen & Cohen (1993) introduce a finite elements method for 3D deformable surface models. Borkowski (2004) shows the capabilities of snakes for break line detection in the context of surface modelling. Laptev et al. (2001) extract roads using a combined scale space and snake strategy.

In order to extract roads from ALS data, Rieger et al. (1999) propose twin snakes to model roads as parallel edges. This integration of model based knowledge stabilises the extraction and is able to bridge gaps in the structure lines in the vicinity of roads, which are often not continuous in nature. Road extraction can also be improved by fusing ALS and image data, e.g. (Zhu et al., 2004), as well as GIS data (Oude Elberink & Vosselman, 2006). The ALS intensity values, assumed to be a by-product a few years ago, can also be exploited in the extraction process. Roads have usually small intensity values and can be distinguished well from other objects by this feature along with the fact that they are situated on the DTM (Alharthy & Bethel, 2003; Clode et al., 2007). ALS data have also been used to detect bridges (Clode et al., 2005; Sithole & Vosselman, 2006).

In our previous work we used network snakes (Butenuth, 2008) for adapting 2D road vector data to ALS intensity and height data (Goepfert & Rottensteiner, 2009). The image energies consisted of a combination of the ALS intensity, the DSM heights, and a smoothness term derived from the DSM. As roads are situated on the terrain, smoothness should be derived from a DTM. Furthermore, using the raw DSM heights for the image energy, the method cannot be applied to areas with undulating terrain. Another problem of the existing method is that it might be negatively affected by buildings and bridges. Buildings sometimes have similar ALS intensities as roads, which in densely built-up areas may cause the snake to be caught in a local minimum. Considering bridges is essential because they have a disturbing effect on the road that passes underneath the other one. By the new definition of the image energy our method should become more generally applicable.

2. METHOD

2.1 General Work Flow

In this paper a top-down method using the concept of network snakes for adapting road networks from ATKIS data base to ALS data is proposed. The initialization of the snake and therefore the internal energy are obtained from the vector data, whereas the ALS information defines the new image energy forcing the snake to salient features (cf. section 2.3). Compared to our previous work (Goepfert & Rottensteiner, 2009), we improve the image energy by terms related to the smoothness of the DTM and by terms derived from building outlines and bridge positions. Extracted buildings are used to act as repulsion forces in the image energy, whereas bridge detection is performed in order to determine confident areas for the correct road position. After defining and weighting the different terms of internal and image energies the iterative optimisation process is started modifying the position of the network snake. The change of the position of the contour in the current iteration is used to determine the convergence of the algorithm. Afterwards, the new position of the contour should match the corresponding features for the road network in the ALS data.

2.2 Snakes and network snakes

It is the general idea of snakes that the position of the contour in an image is determined in an iterative energy optimisation process. An initialisation of the contour is required. Three energy terms are introduced by Kass et al. (1988). The internal energy E_{int} defines the elasticity and rigidity of the curve. The image energy E_{image} should represent the features of the object of interest in an optimal manner in order to attract the contour step by step to the desired position. Additional terms (constraint energy E_{con}) can be integrated in the energy functional forcing the contour to fulfil predefined external constraints:

$$E^*_{snake} = \int_0^1 (E_{\text{int}}(v(s)) + E_{image}(v(s)) + E_{con}(v(s)))ds \quad (1)$$

where $v(s) = (x(s), y(s))$ is the parametric curve with arc length s. In order to obtain the optimal position of the snake in the image, the energy functional in Equ. 1 has to be minimised, e.g. by variational calculus. The internal energy can be written as (Kass et al., 1988):

$$E_{\text{int}}(v(s)) = \frac{\alpha(s)\cdot|v_s(s)|^2 + \beta(s)\cdot|v_{ss}(s)|^2}{2} \quad (2)$$

where v_s and v_{ss} are the derivatives of v with respect to s, and α and β are weights. The first order term, weighted by α, is responsible for the elasticity of the curve. Due to the arc length minimizing effect, high values of α result in very straight curves. The second order term, weighted by β, forces the snake to act like a thin plate and determines the rigidity of the curve. High values of β cause a smooth curve while contour parts with a small β are able to model the behaviour of corners. Using the idea of network snakes (Butenuth, 2008) allows exploiting the initial topology of a network of lines during the energy minimisation process. The individual lines of the network are connected via nodes of an order higher than two at the junctions of these lines. The internal energy has to be modified so that this initial topology is preserved in the resulting line network. This means that at junctions, the elasticity term in Equ. 2 is disregarded ($\alpha = 0$), whereas there is one smoothness term (weighted by β) per line intersecting at the junction node (Butenuth, 2008). The image energy has to be defined in a way to ensure that the snake is attracted to image features that are characteristic for the object to be extracted. Thus, model knowledge is to a large degree incorporated into the image energy. Our new definition for the image energy, including the integration of a building mask, the extraction of bridges, and planar features in the DTM is explained in Section 2.3. We do not use any constraint energy terms in our method.

2.3 Image energy

The image energy E_{image} consists of three different components, namely a general ALS energy E_{ALS}, a building term E_{build} that repulses the snakes from buildings, and a bridge term E_{bridge} attracting the snake to bridges detected in the ALS data:

$$E_{image} = \kappa_I \bullet [\lambda(x,y) \bullet E_{ALS} + \mu(x,y) \bullet E_{build} + \nu(x,y) \bullet E_{bridge}] \quad (3)$$

In Equ. 3, κ_I is a weight for the entire image energy term, and $\lambda(x,y)$, $\mu(x,y)$, and $\nu(x,y)$ are weight functions for the individual terms that may vary over the image. More specifically, our method requires the detection of buildings and bridges. Let *Build(x,y)* be a binary image that takes a value of 1 to indicate the presence of a building and 0 otherwise. Analogously, let *Bridge(x,y)* be a binary image indicating the presence of a bridge. Then we define

$$\begin{aligned} \lambda(x,y) &= \lambda_0 \bullet [1 - Build(x,y)] \bullet [1 - Bridge(x,y)] \\ \mu(x,y) &= \mu_0 \bullet Build(x,y) \\ \nu(x,y) &= \nu_0 \bullet Bridge(x,y) \end{aligned} \quad (4)$$

with $\lambda_0 = \mu_0 = \nu_0 = 1 = const$. In other words, in regions classified as a building, only E_{build} is taken into account, in regions classified as a bridge only E_{bridge} is considered, and in all other areas only E_{ALS} is used. In the subsequent sections, we will describe the individual energy terms in more detail.

2.3.1 General ALS Energy: The general ALS energy E_{ALS} requires an intensity image and a DTM, which have to be generated from the ALS point cloud in a pre-processing stage. The intensity image is interpolated by means of kriging (Cressie, 1990). Then it is smoothed by a median filter in order to remove outliers as well as decrease the noise while preserving the road edges. In order to determine a DTM, the ALS points have to be classified as terrain or off-terrain points. In order to achieve this classification, we estimate a plane for each point, taking into account its *k* (e.g., 9) nearest neighbours. Taking the RMS error of the weight unit of the planar fit as a measure for the local surface roughness, we search for connected segments of points that have a low surface roughness. Using a morphological opening filter, a coarse DTM is generated from the DSM (Weidner & Förstner, 1995), and each segment is classified according to its average height difference from the approximate DTM. An improved DTM can be generated from the points in segments classified as terrain segments, and the classification can be repeated taking advantage of the improved DTM from the first iteration. In order to also include terrain points that are characterised by a high surface roughness, a final classification of all ALS points is carried out based on their height differences from the improved DTM. The DTM grid is interpolated taking into account only the terrain points. It is important to note that this method will classify points on bridges as ground points, because the road will correspond to a large segment that is situated on the terrain everywhere except at the bridge.

The general ALS energy E_{ALS} is composed of the weighted sum of the intensities and plane parameters in the DTM:

$$E_{ALS} = a \cdot E_I + b \cdot E_{Plane} \quad (5)$$

where E_I is the energy from intensity image, E_{Plane} is the energy from the plane parameters, and *a, b* are weights. Intensity values of the ALS data represent the reflectance properties of the illuminated objects according to the wavelength of the emitted beam (near infrared). Road surfaces such as asphalt generally appear dark due to the high absorption rate (Clode et al., 2007). Therefore, the pre-processed intensity image determines the first term E_I in Equ. 5, forcing the snake to low grey values. However, some other objects such as building roofs show a similar behaviour and disturb the optimization process related to E_I. The term E_{Plane} in Equ. 5 exploits the fact that roads are usually situated on smooth and flat surfaces. Therefore, a plane is estimated in a 5 m x 5 m window for every grid point in the DTM, thus considering common values of the road width. The term E_{Plane} is the sum of the absolute values of the plane slope in x- and y-direction. E_{Plane} thus highlights strong slopes in every direction in the image energy. This energy part should prevent that roads represented by the snakes move to surface areas which have invalid height gradients. The weights (*a*, *b)* of the energy parts in Equ. 3 are determined empirically supported by the histograms of the images.

2.3.2 Building Energy: The second component E_{build} in Equ. 3 is dedicated to buildings. Due to different roof orientation and materials the appearance of buildings in the Lidar intensities varies considerably. This fact results in many undesired edges and local minima in the energy part derived from the intensity. Furthermore, buildings cause strong edges in the DSM and even in the DTM some artefacts remain, disturbing a suitable energy definition for the adaptation of roads using active contours. On the other hand buildings have strong relations to the adjacent road segments: they can be treated as forbidden areas for standard roads, acting as a repulsion force.

In order to take advantage of building information for our purposes, the buildings have to be detected in the ALS data in a pre-processing stage. We use the method described in (Rottensteiner et al., 2007) for that purpose. For the definition of the energy term E_{build}, we only need a binary building mask. A distance transform is applied to the building mask, and the binary image *Build(x,y)* used to define the weight $\mu(x,y)$ of E_{build} (Equ. 4) is generated by thresholding the distance image at 4 m (8 pixels). Thus, E_{build} will be effective inside the building and within a distance of 4 m from the building boundary. The building energy E_{build} itself is based on a distance transform of the negation of the binary image *Build(x,y)*. That is, E_{build} is zero outside the enlarged building area described by *Build(x,y)*, whereas in the interior of a building it is identical to the distance to the nearest non-building pixel. The skeletons of the building areas act as decision boundaries. If the initialisation of the road network is situated on the correct side of the building skeleton the snake will slide to the sufficient urban "valley". Fig. 1 visualises a part of the image energy without considering bridges, i.e. using *Bridge(x,y)* = 0 for all pixels.

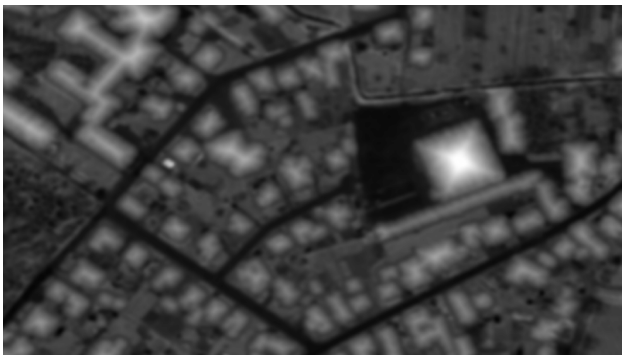

Figure 1. Image energy without bridges.

2.3.3 Bridge energy: Due to the fact that bridges indicate the course of roads with high confidence, the information about this object class should guide the evolvement of the snake in the corresponding areas. Therefore, a method is proposed that estimates the width, length, direction, and the position of the bridge centre in the DTM and converts this information into a suitable image energy term for the related nodes of the road network. In this context, it is important that our DTM filtering method will assign the bridge to the terrain (cf. section 2.3.2).

The approximate positions of bridges are usually stored in attributes of the corresponding ATKIS road objects. Otherwise, the approximate positions can be detemined by intersecting road segments with other objects (e.g., larger rivers or railways) or by finding road crossings without common nodes of the different road segments, assuming the topology of the ATKIS data to be correct. Our bridge detection method starts with the determination of the direction and the width of a bridge. We assume the terrain to be smooth because buildings, trees, and similar objects have already been removed. As a consequence, bridges will have the strongest edges in the DTM. An edge amplitude image is generated from the DTM in the vicinity of the approximate bridge position (e.g., 100 m x 100 m) by convolving it by a Sobel operator. We generate the histogram of this amplitude image and determine the largest amplitude corresponding to a local minimum in a smoothed version of the histogram. This amplitude is used as a threshold to mark edge pixels (Fig. 2a). They are assumed to belong to the bridge borderline and are transferred to the Hough space for straight lines. We determine the maximum in Hough space. It is supposed to correspond to one of the edges of the bridge, and its line direction thus corresponds to the direction of the bridge. The second edge of the bridge should correspond to a relative maximum in Hough space having the same direction, but a different offset (Fig. 2b). This relative maximum is searched for, using information about suitable bridge widths to restrict search space. If no relative maximum is found at this line direction, i.e. if the second highest entry in the Hough space is smaller than half the maximum, the procedure is abandoned and the bridge information is not taken into account. Otherwise, the offset difference between the two maxima should correspond to the bridge width. The width and the direction of the bridge are then used to design a template in order to determine the coordinates of the bridge centre in the DTM by area-based matching. The template models the bridge to connect two horizontal planes that are separated by a trapezoidal valley (Fig. 2c). The length of the bridge is estimated by the maximum extent of the segmented edge pixels corresponding to the longer bridge borderline. The trapezoidal shape of the "valley" in the template should alleviate the fact that the length of the bridge thus determined is not very accurate. The bridge template is moved over the DTM, and the cross correlation coefficient is determined at each position. A small area around the maximum of the correlation image is segmented by thresholding (Fig. 2d), and this area is used for a distance transform (Fig. 2e). E_{bridge} is determined by shifting the results of the distance transform in the bridge direction. More precisely, for any node k on the bridge (according to the bridge length) having the coordinates (x,y), E_{bridge} is defined as

$$E_{bridge}(x,y) = d[x + (k\text{-}c) \bullet \Delta s \bullet \Delta x,\ y_0 + (k\text{-}c) \bullet \Delta s \bullet \Delta y] \qquad (6)$$

In Equ. 6, c is the node index of the pixel in the centre of the bridge, $(\Delta x, \Delta y)$ is the (normalised) direction vector of the bridge, Δs is the nominal spacing of nodes in the snake and $d(x,y)$ is the result of the distance transform. In case of two intersecting roads, for the underpass this energy is only used for the central node, i.e. for the node directly under the bridge. The binary image of bridge pixels $Bridge(x,y)$ used to define the weights $v(x,y)$ (cf. Equ. 4) thus is zero everywhere except in a narrow band of a few pixels width to the left and to the right of the approximate position of the snake from the last snake node before the bridge to the first node after the bridge. This implies that $Bridge(x,y)$ is updated after each iteration in the optimisation process. Although the inverse correlation image could already be used for E_{bridge}, the distance transform modifies this information to a more continuous and homogeneous force field. The extracted bridge points could also act as anchor points for spring forces attracting the snake to the desired position similar to the suggested strategy in (Kass et al., 1988). However, such a strategy would introduce an additional constraint energy term and, thus, new weights, which make the fine-tuning of the parameters more complex.

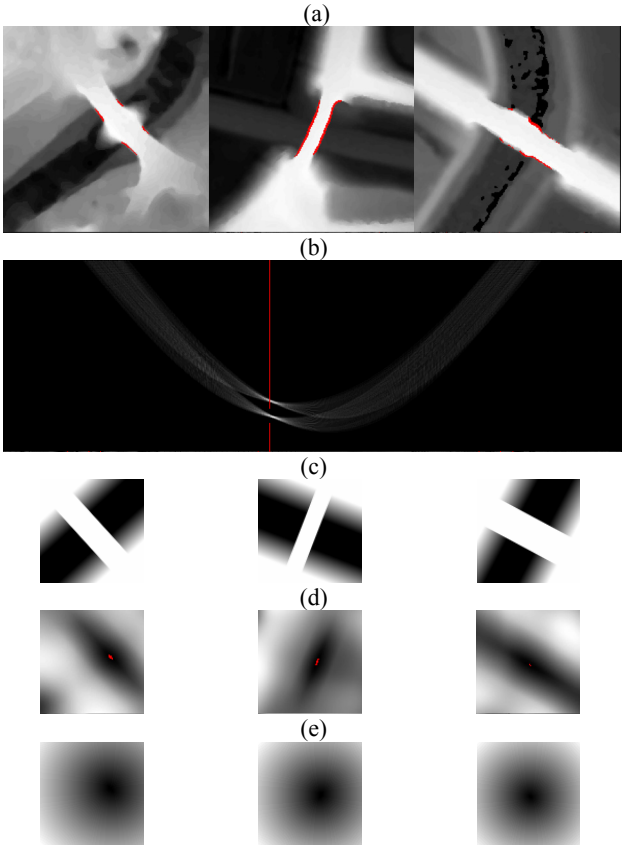

Figure 2. (a) Bridge borderlines in the DTM; (b) search for the second parallel borderline in the Hough space (red: bridge direction); (c) bridge templates; (d) inverse correlation image (red: minimum); (e) E_{bridge} of the central bridge node after distance transform.

3. EXPERIMENTS

3.1 Data

The ALS data set was acquired by the company TopScan during a countywide flight campaign of Schleswig-Holstein between 2005 and 2007. Flying at an altitude of 1000 m the system ALTM 3100 from Optech was used in the first and last echo mode to provide an overall point density of 3-4 points/m^2 and a required accuracy of 0.15 m (height) and 0.3 m (position). From the ALS data a DTM and an intensity grid of 0.5 m resolution are interpolated using the methods described in Section 2.3.1. The ATKIS vector data set (road network only) was manually adapted to orthophotos in order to create reliable ground truth. Afterwards the position was shifted by different distances in several directions to simulate the inconsistent ATKIS data base which is used for initialisation in our analysis.

3.2 Results

The first four examples adapt a small road network in the vicinity of one bridge both without and with the bridge energy

E_{bridge} in order to show the benefits of using this information (Figs. 3). The weights used in this and all the following examples are given in Tab. 1; these values were determined empirically. Tab. 2 and 3 illustrate the RMS of the point to line distances of the results for the four examples shown in Fig. 3. Generally, if the initialisation is located within the borderline of the bridge the quality of the results without bridge information is similar to the other. However, the algorithm converges faster with the integration of the bridge detection method. If the initial position of the road network is situated outside the bridge due to large differences between the landscape model and the height data the snake is not able to jump across the strong edges along the bridge using only E_{ALS} and E_{build} and thus can not move to the correct position. However, in all examples in Fig. 3 the bridge energy supports the adaptation of the small road network in such a manner that the snake reaches a suitable position.

parameter	α	β	κ_I
value	0.1	0.2	5

Table 1: Weights for the different energy terms of the snakes for all illustrated examples.

RMS of point to line distances (m)	Bridge 1		Bridge 2	
	without	with	without	with
Initialisation	8.24	8.24	5.63	5.63
Solution	6.00	0.61	3.95	1.87

Table 2: Evaluation of the results in examples 1 and 2.

RMS of point to line distances (m)	Bridge 3		Bridge 4	
	without	with	without	with
Initialisation	4.84	4.84	5.11	5.11
Solution	3.77	2.13	2.42	2.06

Table 3: Evaluation of the results in examples 3 and 4.

In the first example (Fig. 3a) a straight road is adapted. For the simulation of inconsistencies the initialisation was shifted by 6 m both in x and y. The results without the bridge energy could be improved by larger weights for the internal energy terms in order to increase the smoothness of the contour. However, this means that other road parts with strong curvature can not be treated without defining different weights for special segments. This would make the algorithm more complex and the transferability to other data sets would suffer. With the bridge information it is much easier to define weights that can be applied to the entire road network. The second and the fourth examples (Figs. 3b and 3d) show a similar behaviour. Each initialisation was shifted by 5 m both in x and y. The integration of the bridge energy significantly improves the quality of the results. Obviously, the bridge energy affects only the network nodes in a certain vicinity. Therefore, the quality improvement in the example 2 is larger (2.08 m) than in example 4 (0.36 m). In the third test the underpass road is not located in the centre of the bridge (cf. DTM in the centre of Fig. 2(a)). Therefore, the assigned new image energy forces this road segment to the bridge centre, which is in this case not the correct position. Thus, a larger RMS difference to the reference (2.13 m) can be observed than in the other examples. For this situation the bridge detection method has to be extended by position and direction information of the underpass road.

Fig. 4 visualises the adaptation of a larger road network including four bridges. The initialisation was again shifted by 5 m in each coordinate axis, resulting in a RMS of the perpendicular point to line distances of 4.88 m. After the optimisation process this value decreases to 2.91 m.

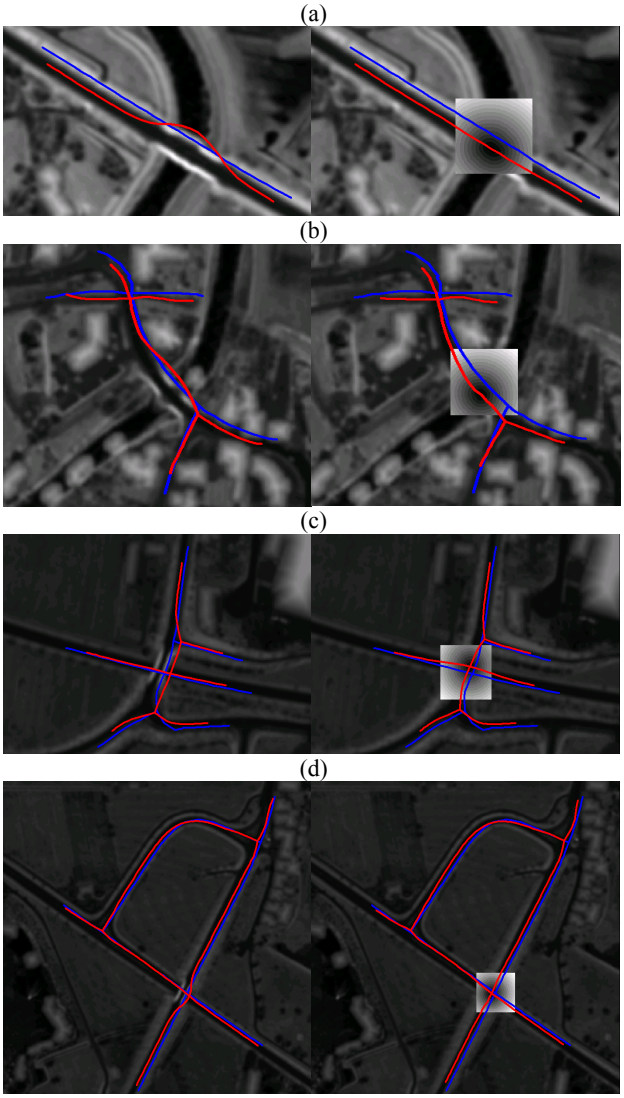

Figure 3. Adaptation of four small road networks to ALS data near single bridges (blue: initialisation; red: final position; left/right: without / with bridge energy.

Figure 4. Adaptation of larger road networks (2199 nodes) to ALS data with bridge energy (blue: initialisation; red: final position).

One of the main problems causing the remaining large differences to the reference is that road parts with strong

curvature are straightened out by the original definition of the internal energy. For our application it would be desirable to modify this energy term in order to preserve the curvature of the initialisation. The current definition of the internal energy causes another drawback. At the moment the smoothness term does not affect road segments linked by a crossing node. Thus, especially at T-junctions the initial shape is inadvertently deformed. For that reason the DLM shape has to be exploited in order to penalise a strong change of the initial shape.

4. CONCLUSION

This paper is focused on the adaptation of road centrelines to ALS data by means of network snakes. The method described in our previous work (Goepfert & Rottensteiner, 2009) is extended in order to exploit building and bridge information. These two objects provide strong features in ALS data. A building mask is used to modify the image energy so that the snake is repulsed from the detected buildings. In order to use the information about bridges in the road adaptation procedure, we had to develop a technique for bridge detection. The bridge information enables the method to deal with poor initialisations situated completely outside the bridge borderlines. The evaluation of our method shows that it gives satisfactory results in the vicinity of strong features in the ALS data, such as buildings and bridges. However, in areas of strong road curvature and weak image energy the smoothing effect of the internal energies can not be compensated. Therefore, in our future work a modification of the internal energy should penalise the change of the initial curvature instead of the deviation from a smooth straight line in order to limit the shape variation. However, this strategy is associated with a higher confidence in the correctness of the initial shape in the ATKIS data base. The loss of the smoothness term at crossings and T-junctions is also not suitable in each situation. In this case the exploitation of information from the initialisation, such as perpendicularity, can be useful, too. The proposed algorithm is only one step in the larger framework developed to solve the inconsistencies between the DLM and height information. All objects in the vector data represented by suitable features in the ALS data should be adapted. This process provides a dense network of shift vectors which can be used in addition to prior accuracy knowledge in order to improve the consistency of the DLM and ALS data.

ACKNOWLEDGEMENT

This research was supported by the surveying authorities of Lower Saxony and Schleswig-Holstein. We also express our gratitude to the mentioned authorities for providing the data.

REFERENCES

Alharthy, A., Bethel, J., 2003. Automated road extraction from Lidar data, *Proc. ASPRS Annual Conference, Anchorage, Alaska,* unpaginated CD-Rom.

Blake, A., Isard, M., 1998. Active contours. *Springer, Berlin Heidelberg New York*, 351 p.

Borkowski, A., 2004. Modellierung von Oberflächen mit Diskontinuitäten. *Habilitation*, TU Dresden, Germany, 91p.

Burghardt, D., Meier, S., 1997. Cartographic displacement using the snake concept. In: Förstner, Plümer (eds.), *Semantic modeling for the acquisition of topographic information from images and maps*, Basel, Birkhäuser Verlag, pp. 59-71.

Butenuth, M., 2008. Network snakes. PhD Thesis, University of Hannover, DGK-C 620.

Clode, S., Rottensteiner, F., Kootsookos, P., 2005. Improving city model determination by using road detection from LIDAR data. *IntArchPhRS* XXXVI (3/W24), pp. 159-164.

Clode, S., Rottensteiner, F., Kootsookos, P, Zelniker, E., 2007. Detection and vectorization of roads from Lidar data, *PE & RS* 73(5*)*, pp. 517-536.

Cohen, L. D., Cohen, I., 1993. Finite element methods for active contour models and balloons for 2-D and 3-D images, *IEEE TPAMI* 15(11), pp. 1131-1147

Cressie, N. A. C., 1990. The origins of Kriging, *Mathematical Geology* 22, pp. 239-252.

Goepfert, J., Rottensteiner, F. 2009. Adaptation of roads to ALS data by means of network snakes: *IntArchPhRS 38-3/W8*:24-29.

Kass, M, Witkin, A, Terzopoulos, D., 1988. Snakes: active contour models. *Int. J. Computer Vision* 1(4):321-331.

Koch, A., 2006. Semantische Integration von zweidimensionalen GIS-Daten und Digitalen Geländemodellen. PhD Thesis, University of Hannover, DGK-C 601.

Laptev, I., Mayer, H., Lindeberg, T., Eckstein, W., Steger, C. Baumgartner, A., 2000. Automatic extraction of roads from aerial images based on scale space and snakes, *Machine Vision and Applications* 12, pp. 23-31.

Lenk, U., 2001. 2.5D-GIS und Geobasisdaten - Integration von Höheninformation und Digitalen Situationsmodellen. PhD Thesis, University of Hannover, DGK-C 546.

McInerney, T., Terzopoulos, D., 1995. Topologically adaptable snakes. *Proc. Int. Conf. Computer Vision*, pp 840-845.

Oude Elberink, S., Vosselman, G., 2006. Adding the third dimension to a topographic database using airborne laserscanning, *IntArchPhRS* XXXVI/3, pp. 92-97.

Pilouk, M., 1996. Integrated modelling for 3D GIS, PhD Thesis, Enschede, The Netherlands, *ITC Publication Series 40*.

Rieger, W., Kerschner, M., Reiter, T., Rottensteiner, F., 1999. Roads and buildings from laser scanner data within a forest enterprise, *IntArchPhRS* XXXII / 3-W14, pp. 185-191.

Rottensteiner, F., Trinder, J., Clode, S., Kubik, K., 2007. Building detection by fusion of airborne laserscanner data and multi-spectral images: Performance evaluation and sensitivity analysis. *ISPRS J. Photogr. & Rem. Sens. 62(2)*: 135-149.

Rousseaux, F., Bonin, O., 2003. Towards a coherent integration of 2D linear data into a DTM, *Proc. 21st International Cartographic Conference (ICC)*. pp. 1936-1942.

Sithole, G., Vosselman, G., 2006. Bridge detection in airborne laser scanner data. *ISPRS J. Photogr. & Rem. Sens.* 61: 33-46.

Weidner, U. and Förstner, W. 1995. Towards automatic building reconstruction from high resolution digital elevation models, *ISPRS J. Photogr. & Rem. Sens.* 50(4): 38–49.

Zhu, P., Lu, Z., Chen, X., Honda, K., Eiumnoh, A., 2004: Extraction of city roads through shadow path reconstruction using laser scanning, *PE & RS* 70 (12): 1433-1440.